Scaling Behavior and Strain Dependence of In-Plane Elastic Properties of Graphene

J. H. Los, A. Fasolino,* and M. I. Katsnelson
Radboud University, Institute for Molecules and Materials, Heyendaalseweg 135, 6525AJ Nijmegen, Netherlands
(Received 19 August 2015; published 5 January 2016)

We show by atomistic simulations that, in the thermodynamic limit, the in-plane elastic moduli of graphene at finite temperature vanish with system size L as a power law $L^{-\eta_u}$ with $\eta_u \simeq 0.325$, in agreement with the membrane theory. We provide explicit expressions for the size and strain dependence of graphene's elastic moduli, allowing comparison to experimental data. Our results explain the recently experimentally observed increase of the Young modulus by more than a factor of 2 for a tensile strain of only a few per mill. The difference of a factor of 2 between the measured asymptotic value of the Young modulus for tensilely strained systems and the value from *ab initio* calculations remains, however, unsolved. We also discuss the asymptotic behavior of the Poisson ratio, for which our simulations disagree with the predictions of the self-consistent screening approximation.

DOI: 10.1103/PhysRevLett.116.015901

Mechanical and structural properties of graphene form an intriguing and highly nontrivial aspect of its physics. The structure of a two-dimensional (2D) material embedded in a 3D space gives room to special features, related to large out-of-plane deformations, in particular, thermal ripples [1–9] and static ripples and wrinkles [10]. A crucial difference with 3D (or strictly 2D) crystals is that, for graphene, out-of-plane atomic displacements h and in-plane displacements $\mathbf{u}$ have different wave vector dependence of the energy cost in the long wavelength limit $q \to 0$, namely $\propto q^2$ and $\propto q$, respectively, the latter being the normal behavior for acoustic phonons. Hence, at finite temperature, the long wavelength out-of-plane fluctuations are much larger than the in-plane ones, so that at some small wave vector q the first anharmonic coupling term of the form uh^2 will dominate over the "normal" harmonic terms u^2, with important consequences for the elastic behavior [8,9,11–14]. In particular, the wave vector dependence of the anharmonic coupling strength leads us to expect a power law scaling of the size dependence of the elastic properties.

Contrary to the temperature dependence [15,16], so far the size dependence of the in-plane elastic moduli of graphene has been neither studied nor measured [17] until recent experiments seem to indicate that such a size dependence does exist for graphene [18–20]. In particular, the recently measured anomalous strong variation of more than a factor of 2 of the Young modulus Y with tensile strain for graphene [19] can be considered as a consequence of size scaling, although direct (experimental) evidence is still lacking. Scaling with size of the bending rigidity κ, predicted by the theory of membranes [11] and atomistic simulations [4] has been instead recently confirmed experimentally [21].

Here we study the size dependence of the in-plane elastic moduli of graphene at room temperature $T = 300$ K by means of atomistic Monte Carlo (MC) simulations based on the realistic interatomic potential LCBOPII [22], as used in previous works [2,4,15]. We obtain explicit expressions for the size and strain dependence of graphene's in-plane elastic moduli, providing a benchmark and tools for the analysis of experiments for systems of any size.

Theoretically, the mentioned size dependence has been studied within the continuum elastic theory of thin plates and membranes, described by the Hamiltonian [23]:

$$H = \frac{1}{2}\int d\mathbf{r}[\kappa(\nabla^2 h)^2 + \lambda u_{\alpha\alpha}^2 + 2\mu u_{\alpha\beta}^2], \tag{1}$$

where $\mathbf{r}$ is the 2D position vector, κ is the bending rigidity, λ and μ are Lamé coefficients, with μ the shear modulus, and

$$u_{\alpha\beta} = \frac{1}{2}(\partial_\alpha u_\beta + \partial_\beta u_\alpha + \partial_\alpha h \partial_\beta h) \tag{2}$$

is the strain tensor.

The harmonic approximation neglects the nonlinear h^2 term, decoupling the bending and stretching modes. Then the correlation functions for out-of-plane displacements $H_0(q) = \langle |h_\mathbf{q}|^2 \rangle_0$ and for in-plane displacements $D_{u,0}^{\alpha\beta}(q) = \langle u_{\alpha\mathbf{q}}^* u_{\beta\mathbf{q}} \rangle_0$ can be derived by Gaussian integration [8,9]:

$$H_0(q) = \frac{k_B T}{\kappa q^4} \tag{3}$$

and

$$D_{u,0}^{\alpha\beta}(q) = \frac{P_{\alpha\beta}(\mathbf{q}) k_B T}{(\lambda + 2\mu) q^2} + \frac{[\delta_{\alpha\beta} - P_{\alpha\beta}(\mathbf{q})] k_B T}{\mu q^2}, \tag{4}$$

with $P_{\alpha\beta}(\mathbf{q}) = q_\alpha q_\beta / q^2$. The average height fluctuation behaves as $\langle h^2 \rangle_0 = \sum_\mathbf{q} \langle |h_\mathbf{q}|^2 \rangle_0 \sim L^2$, implying instability of a membrane as a flat phase.

Because of the large out-of-plane fluctuations, however, the harmonic behavior is not valid for small q and one has to keep the h^2 term in Eq. (2). Since H remains quadratic in u, these degrees of freedom can still be integrated out. This leads to a Hamiltonian in Fourier space which is a function of $h_{\mathbf{q}}$ only [9]:

$$\tilde{H} = \frac{1}{2}\sum_{\mathbf{q}} \kappa q^4 |h_{\mathbf{q}}|^2 + \frac{Y}{8}\sum_{\mathbf{q},\mathbf{k},\mathbf{k}'} R(\mathbf{q},\mathbf{k},\mathbf{k}') h_{\mathbf{k}} h_{\mathbf{q}-\mathbf{k}} h_{\mathbf{k}'} h_{-\mathbf{q}-\mathbf{k}'}, \tag{5}$$

where Y is the 2D Young modulus and $R(\mathbf{q},\mathbf{k},\mathbf{k}') = (\mathbf{q}\times\mathbf{k})^2(\mathbf{q}\times\mathbf{k}')^2/q^4$. The anharmonic, quartic term reduces the height fluctuations, stabilizing the flat phase, effectively described by a renormalized bending rigidity $\kappa_R(q) \sim q^{-\eta}$ with positive η. Hence, the height correlation $H(q)$ for $q \to 0$ has the same form as $H_0(q)$ in Eq. (3), but with κ replaced by $\kappa_R(q)$ [11]. Likewise, $D_u^{\alpha\beta}(q)$ can be described by renormalized $\lambda_R(q), \mu_R(q) \sim q^{\eta_u}$ in Eq. (4) with $\eta_u > 0$. From rotational invariance it follows that η and η_u should satisfy the scaling relation $\eta_u = 2 - 2\eta$ [24].

Within the self-consistent screening approximation (SCSA) [13], the exponent η was estimated to be 0.821 [13]; next-order corrections reduce it slightly to $\eta \simeq 0.789$ [14]. A renormalization group approach gives $\eta = 0.849$ [25] and MC simulations for self-avoiding membranes $\eta \simeq 0.72$ [26]. With $\eta > 0$, $\langle h^2\rangle \sim L^{2-\eta}$ is much smaller than $\langle h^2\rangle_0 \sim L^2$ for large L, stabilizing the flat phase.

Although it is *a priori* not obvious whether the membrane theory applies to an atomic-layer-thick 2D crystal like graphene, atomistic MC simulations confirm the scaling behavior of $H(q)$ with $\eta \simeq 0.85$ [4]. Also recent experiments confirm the scaling of κ [21]. The scaling of in-plane elastic moduli, instead, has not yet been studied or confirmed for graphene. Contrary to κ_R which increases with increasing system size, making the membrane more resistant against bending, λ_R and μ_R decrease with system size. Hence, if graphene follows the membrane theory, the in-plane elastic moduli vanish for large system sizes, an unthinkable situation for 3D crystals.

For a 2D system, the 2D bulk modulus B, the uniaxial elastic modulus C_{11} and Y are related to λ and μ as

$$B = \lambda + \mu, \qquad C_{11} = B + \mu, \quad \text{and} \quad Y = \frac{4B\mu}{B+\mu}, \tag{6}$$

implying that B, C_{11}, and Y scale as λ and μ. A related, but not scaling, quantity is the 2D Poisson ratio ν:

$$\nu = \frac{B-\mu}{B+\mu}. \tag{7}$$

The SCSA predicts a universal, negative Poisson ratio $\nu = -1/3$ for $L \to \infty$ [13], later confirmed by MC simulation of self-avoiding membranes [27]. For graphene, however, so far only positive values were reported ($\nu = 0.15$–0.46) [15,28,29] but the limit $L_0 \to \infty$ has not yet been studied.

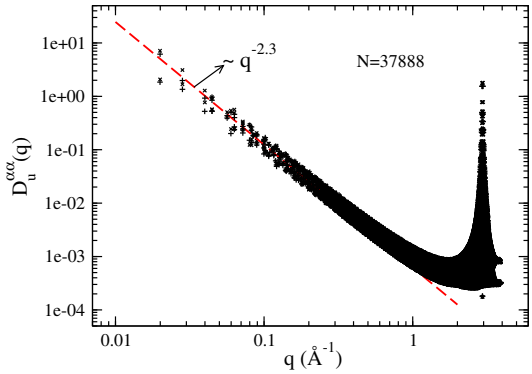

FIG. 1. Correlation functions $D_u^{\alpha\alpha}(\alpha = x, y)$ for in-plane displacements u_{ix} (**x**) and u_{iy} (+). The scaling exponent is consistent with $D_u^{\alpha\alpha} \sim q^{-2-\eta_u}$ with $\eta_u = 2 - 2\eta = 0.3$, using $\eta \simeq 0.85$ [25] (dashed line).

In Fig. 1 we show the in-plane correlation function $D_u^{\alpha\alpha}(q)(\alpha = x, y)$ obtained from MC simulations within the NPT ensemble (NPT MC) at pressure $P = 0$ and $T = 300$ K applying isotropic 2D volume fluctuations. A roughly square system with $N = 37888$ atoms and periodic boundary conditions was used. Besides the usual atomic displacement moves we apply also collective wave moves for small q as in Ref. [4], reducing substantially the required computation time, which was of the order of 10^6 cycles in this case (1 cycle corresponds N single atom move trials). For the calculation of $D_u^{\alpha\alpha}(q) = \langle|u_q^\alpha|^2\rangle = (1/N)\langle|\sum_i^N u_{i\alpha}\exp(i\mathbf{q}\mathbf{r}_{i,0})|^2\rangle$ with $\{r_{i,0}\}$ the ground state positions, the in-plane displacement field was computed as $u_{i\alpha} = s r_{i\alpha} - r_{i\alpha,0}$, where $s = \sqrt{A_0/A}$ scales the area A at $T = 300$ K to the ground state area A_0 of a flat sample. The behavior of $D_u^{xx}(q)$ for small q is consistent with a power law with exponent $\eta_u \simeq 0.3$, indicating that for graphene also λ and μ follow the membrane theory.

The size and strain dependence of the bulk modulus can be obtained simultaneously by NPT simulations for different sizes with isotropic area fluctuations at several pressures P. The resulting average area A gives the equation of state (EOS), $A(P)$ and thus $P(A)$, from which B can be calculated as:

$$B = -A\frac{\partial P}{\partial A} = -\frac{s}{2}\frac{\partial P}{\partial s} \tag{8}$$

where $s = L/L_0$ is the relative linear system size with $L_0 = \sqrt{N/\rho_0}$ the ground state system size, $\rho_0 \simeq 0.3819$ Å^{-2} being the 2D ground state atomic density of graphene. To obtain both B and C_{11}, we also performed NPT simulations for uniaxial pressure P_x, applying fluctuations of L_x in the x-direction, while keeping L_y fixed. Then C_{11} follows from:

$$C_{11} = -L_x\left.\frac{\partial P_x}{\partial L_x}\right|_P = -s_x\left.\frac{\partial P_x}{\partial s_x}\right|_P \simeq -s_x\left.\frac{\partial P_x}{\partial s_x}\right|_{s_y = s_{\text{eq}}} \tag{9}$$

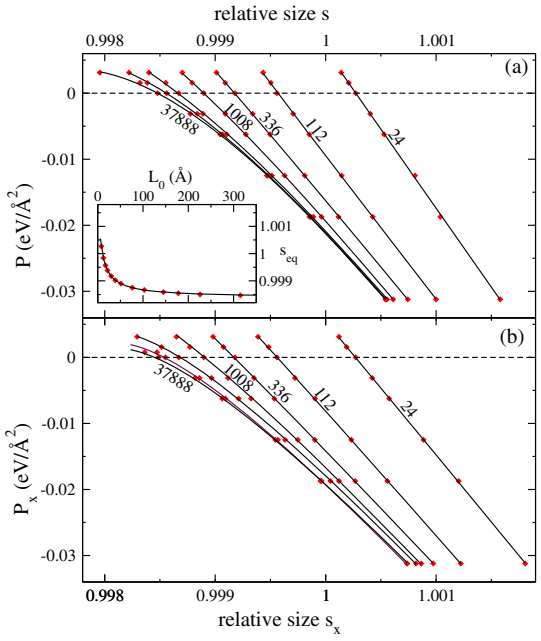

FIG. 2. Pressure as a function of size in NPT simulations (symbols) with (a) isotropic and (b) uniaxial size fluctuations for approximately square systems with $N = 24$, 112, 336, 1008, 4032, 12096 and 37888 atoms. The lines are best fits to Eq. (11). The inset gives the equilibrium sizes $s_{\rm eq} = s(P = 0)$ (symbols) as a function of L_0 and the fit (solid line) according to the expression in Table I.

where $s_\alpha = L_\alpha/L_{\alpha,0}$, with $L_{\alpha,0}(\alpha = x, y)$ the ground state dimensions, and where $s_{\rm eq} = s(P = 0)$ is the equilibrium size obtained from the isotropic NPT simulations at $P = 0$. The subscript "P" in Eq. (9) indicates that L_y should be taken equal to $s_y = s(P)$ resulting from isotropic NPT simulations at pressure P and that P_x should be varied around P. However, since we verified that the dependence of $\partial P_x/\partial s_x$ on s_y is very weak we adopted the last approximation in Eq. (9), which is exact for $P = 0$.

The results are shown in Fig. 2. The inset shows that the previously found negative thermal expansion [15] is also size dependent, but tending to a constant for large L_0. On the basis of Fig. 2(a), with the slope $\partial P/\partial s = 2B/s$ tending to a constant for large s, we propose the following phenomenological relation for $B(s)$

$$B(s) = \frac{s[B_{\rm eq}/s_{\rm eq} + CD(s - s_{\rm eq})]}{1 + D(s - s_{\rm eq})}, \qquad (10)$$

where $B_{\rm eq}$ is the equilibrium value at $P = 0$. Substitution of Eq. (10) into Eq. (8) and integration yields the equation of state

$$P(s) = -\frac{2}{D}\left(\frac{B_{\rm eq}}{s_{\rm eq}} - C\right)\ln\left[1 + D(s - s_{\rm eq})\right] - 2C(s - s_{\rm eq}). \qquad (11)$$

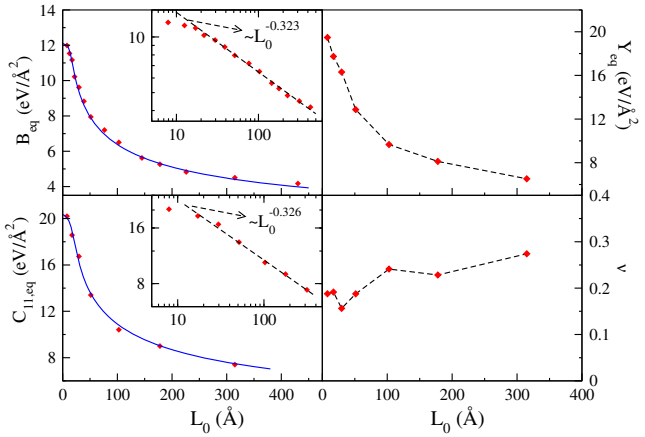

FIG. 3. Left panels: equilibrium bulk modulus $B_{\rm eq}$ and uniaxial modulus $C_{11,\rm eq}$ as a function of L_0. The insets in log-log scale demonstrate the power law behavior. The solid lines are fits according to the expressions in Table I. Right panels: Young modulus $Y_{\rm eq}$ and Poisson ratio ν as a function of L_0. The dashed lines are guides to the eye.

Similarly, we write

$$C_{11}(s_x) = \frac{s_x[C_{11,\rm eq}/s_{\rm eq} + \tilde{C}\,\tilde{D}(s_x - s_{\rm eq})]}{1 + \tilde{D}(s_x - s_{\rm eq})}, \qquad (12)$$

which substituted in Eq. (9) gives an equation for $P_x(s_x)$ similar to Eq. (11) but with s, $B_{\rm eq}$, C, and D replaced by s_x, $C_{11,\rm eq}/2$, $\tilde{C}/2$, and $\tilde{D}$. This form allows the excellent fits shown in Fig. 2, providing $B_{\rm eq}$ and $C_{11,\rm eq}$ as a function of L_0. In the left panels of Fig. 3 we show that both B and C_{11} vanish for large L_0, decreasing as a power law $\sim L^{-\eta_u}$, with $\eta_u \simeq 0.325$ (insets). The right panels give the corresponding results for Y and ν at $P = 0$, calculated using Eqs. (6) and (7). Note that, according to LCBOPII, the in-plane elastic moduli of graphene at $T = 0$ K are $B = 12.69$ eV/Å^2 and $\mu = 9.26$ eV/Å^2, yielding $Y = 21.41$ eV/Å^2 $= 343$ N/m and $\nu = 0.156$, in agreement with *ab initio* data [30] and with the small size limit in Fig. 3 where $Y \simeq 314$ N/m and also with the experimental phonon spectrum of graphite [31,32]. By simulations at 1 K for $N = 24$ we verified that the remaining difference is due to temperature.

Interestingly, the power law decrease of B, C_{11}, and $Y_{\rm eq}$ as a function of L_0 sets in from $L_0 \simeq 20$ Å, a value twice smaller than the Ginzburg critical value $L^* = 2\pi\sqrt{16\pi\kappa^2/(3Yk_BT)} \simeq 40$ Å (using $\kappa \simeq 1.1$ eV [2]) expected from membrane theory [11]. The Poisson ratio ν for small sizes is close to its bare value and increases up to 0.275 for larger L_0, against the SCSA prediction $\nu = -1/3$. Since the scaling of B and μ is consistent with the SCSA, it is very unlikely that ν will reach the value $-1/3$ for $L_0 \to \infty$, as the outcome of Eq. (7) only depends on the prefactors. We remark that $\nu = -1/3$ in Eqs. (6) and (7) leads to $B_R = -\lambda_R$ and $\lambda_R = 2B_R - C_{11}$, implying that λ_R

TABLE I. Size dependent parameters for $B(s)$ and $C_{11}(s_x)$ according to Eqs. (10) and (12) for L_0 in Å. B_{eq}, $C_{11,eq}$, C, and $\tilde{C}$ are in eV/Å^2; other quantities are dimensionless.

$s_{eq} = 0.99838 + [4.295\,10^{-3}/(1 + 0.1814 L_0^{0.94})]$, $D = [(592.3 + 1.25\,10^{-2} L_0^2)/(1 + 1.25\,10^{-5} L_0^2)]$,
$B_{eq} = \{[12.1 - 5.69\,10^{-3} L_0^2 + 28.6(L_0/14.14)^4 L_0^{-0.325}]/[1.0 + (L_0/14.14)^4]\}$, $C = 12.1$,
$C_{11,eq} = \{[20.35 - 7.597\,10^{-3} L_0^2 + 1.47\,10^{-4} L_0^3 + 48.1(L_0/31.62)^4 L_0^{-0.325}]/[1.0 + (L_0/31.62)^4]\}$,
$\tilde{C} = 20.35$, $\tilde{D} = [(309.2 + 0.1597 L_0^2)/(1 + 1.45\,10^{-4} L_0^2)]$, $s_x(s) = 1.15(s - s_{eq}) + s_{eq}$

should be negative for stability while from Fig. 3 one can deduce that $2B_R - C_{11,R}$ remains positive for any L_0.

We can also calculate Y as a function of tensile strain, using Eqs. (10) and (12) with the best fit parameters. We should use the $B(s)$ and $C_{11}(s_x)$ at equal pressure by solving $P_x(s_x) = P(s)$ for s_x at given s. Because of the approximation in Eq. (9), $s_x \neq s$ unless $s = s_{eq}$. An approximation of $s_x(s)$ is given in Table I. The $Y(s)$ obtained from the data of Fig. 2 are shown in Fig. 4 for different sizes. Symbols mark the results at $s = s_{eq}$. Notice the low value of $Y(s_{eq})$ and the strong increase of $Y(s)$ with s for large systems. For example, for $N = 37888$ ($L_0 \simeq 315$ Å), Y increases from $\sim 100\ N/\mathrm{m}$ at $s_{eq} \simeq 0.9985$ to 220 N/m at $s = 0.9995$, i.e., more than a factor 2 for a strain $\epsilon = s - s_{eq} = 0.001$ (0.1%). This strong dependence is in agreement with the recent experiments [18,19].

Since B_{eq} and $C_{11,eq}$, as well as s_{eq}, C, D, $\tilde{C}$, and $\tilde{D}$ turn out to depend smoothly on L_0, we can approximate all parameters by functions of L_0 given in Table I. These expressions, yielding appropriate asymptotics with C ($\tilde{C}$) equal to $\partial P/\partial s$ ($\partial P_x/\partial s_x$) for the smallest system ($N = 24$), enable us to determine the elastic moduli for any system size. The inset of Fig. 4 shows the resulting $Y(s)$ for a size $L_0 = 1\ \mu$m ($\sim N = 3.8 \times 10^7$ atoms). At zero strain (symbol) Y is only 30 N/m, becoming almost a factor of 10 larger at only 0.5% tensile strain, where it approaches its asymptotic value.

Finally, the size dependence of Y with tensile strain at negative pressures is displayed in Fig. 5. A tensile stress of 0.05 N/m, corresponding to $\sim$0.05% strain, suppresses the anharmonic effects, and thus the power law decay, for $L_0 > 0.25\ \mu$m. As a consequence, Y is a factor $\sim$4 larger than Y_{eq} for a system of 1 μm. Subsequently, increasing the stress by a factor of 8 yields a strain of $\sim$0.20% and $Y \simeq 240\ N/\mathrm{m}$.

The strong variation of Y with strain that we find corresponds to recent experimental data [19]. However, the factor of 2 difference in the upper bound of Y, with a reported experimental value $Y = 700\ N/\mathrm{m}$, well above the commonly accepted bare value $Y = 340\ N/\mathrm{m}$ [17,30] reproduced by LCBPOII, remains unexplained and requires further investigation. It should be noted that the experimental values are indirectly determined via the Schwerin equation [17,33], which is derived from the Föppl–von Kármán equations without considering the scaling behavior found here [34]. Possibly, this might be the cause of overestimated experimental values.

In conclusion, we have shown by atomistic simulations that the in-plane elastic moduli of graphene vanish with size as $L_0^{-\eta_u}$ with $\eta_u \simeq 0.325$, confirming that graphene follows the scaling predicted by membrane theory. By combining this with the strain dependence, we provide an explanation for the anomalous strong variations with strain in recent

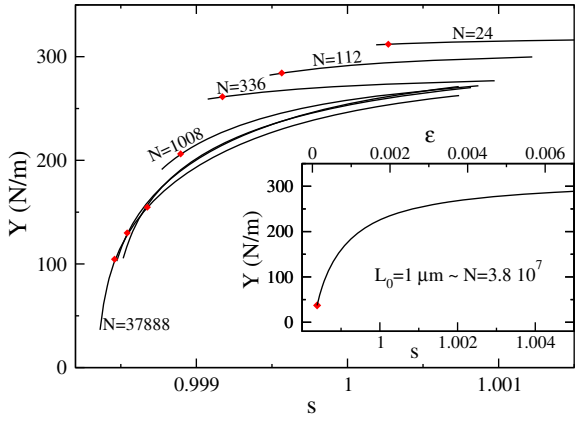

FIG. 4. Young modulus $Y(s)$ as a function of s for sample sizes as in Fig. 2 with symbols for $s = s_{eq}$. The inset shows $Y(s)$ for a size of 1 μm($N \simeq 3.8 \times 10^7$), calculated using Eqs. (10) and (12) and the expressions in Table I. The upper axis of the inset gives the strain $\epsilon = s - s_{eq}$.

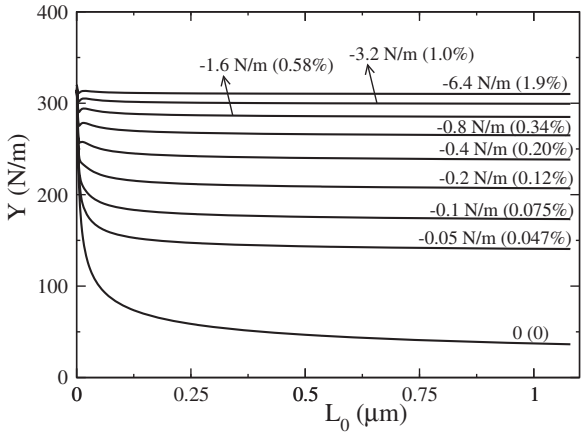

FIG. 5. Young modulus Y as a function of L_0 for the indicated values of the pressure P. The value in brackets is the corresponding strain $\epsilon = s - s_{eq}$.

measurements of the elastic moduli. For reasons of universality, the scaling behavior of elastic properties found here for graphene should apply to all 2D crystals. In contrast, our results do not support the SCSA prediction $\nu = -1/3$ for $L \to \infty$, suggesting that this issue has to be reconsidered within membrane theory. We argue that the demonstrated scaling behavior, implying a nonlocal relation between strain and stress, requires reconsideration of the validity of the Föppl–van Kármán equations for 2D crystals.

This research has received funding from the European Union Seventh Framework Programme under grant agreement No. 604391 Graphene Flagship. We are thankful to Kirill Bolotin for informing us on the recent experimental data in Ref. [20] before publication and to Rafael Roldán for useful discussions.

*a.fasolino@science.ru.nl

[1] J. C. Meyer, A. K. Geim, M. I. Katsnelson, K. S. Novoselov, T. J. Booth, and S. Roth, Nature (London) **446**, 60 (2007).
[2] A. Fasolino, J. H. Los, and M. I. Katsnelson, Nat. Mater. **6**, 858 (2007).
[3] N. Abedpour, M. Neek-Amal, R. Asgari, F. Shahbazi, N. Nafari, and M. R. R. Tabar, Phys. Rev. B **76**, 195407 (2007).
[4] J. H. Los, M. I. Katsnelson, O. V. Yazyev, K. V. Zakharchenko, and A. Fasolino, Phys. Rev. B **80**, 121405 (R) (2009).
[5] R. C. Thompson-Flagg, M. J. Moura, and M. Marder, Europhys. Lett. **85**, 46002 (2009).
[6] R. Zan, C. Muryn, U. Bangert, P. Mattocks, P. Wincott, D. Vaughan, X. Li, L. Colombo, R. S. Ruoff, B. Hamilton, and K. S. Novoselov, Nanoscale **4**, 3065 (2012).
[7] W. Gao and R. Huang, J. Mech. Phys. Solids **66**, 42 (2014).
[8] M. I. Katsnelson and A. Fasolino, Acc. Chem. Res. **46**, 97 (2013).
[9] M. I. Katsnelson, *Graphene: Carbon in Two Dimensions* (Cambridge University Press, Cambridge, 2012), Chap. 9.
[10] W. Zhu, T. Low, V. Perebeinos, A. A. Bol, Y. Zhu, H. Yan, J. Tersoff, and P. Avouris, Nano Lett. **12**, 3431 (2012).
[11] *Statistical Mechanics of Membranes and Surfaces*, edited by D. R. Nelson, T. Piran, and S. Weinberg (World Scientific, Singapore, 2004).
[12] D. R. Nelson and L. Peliti, J. Phys. (Paris) **48**, 1085 (1987).
[13] P. Le Doussal and L. Radzihovsky, Phys. Rev. Lett. **69**, 1209 (1992).
[14] D. Gazit, Phys. Rev. E **80**, 041117 (2009).
[15] K. V. Zakharchenko, M. I. Katsnelson, and A. Fasolino, Phys. Rev. Lett. **102**, 046808 (2009).
[16] S. Chen and D. C. Chrzan, Phys. Rev. B **84**, 195409 (2011).
[17] C. Lee, X. Wei, J. W. Kysar, and J. Hone, Science **321**, 385 (2008).
[18] G. López-Polín, C. Gómez-Navarro, V. Parente, F. Guinea, M. I. Katsnelson, F. Pérez-Murano, and Julio Gómez-Herrero, Nat. Phys. **11**, 26 (2015).
[19] G. López-Polín, M. Jaafar, R. Roldán, C. Gómez-Navarro, and J. Gómez-Herrero, arXiv:1504.05521.
[20] R. J. T. Nicholl, H. J. Conley, N. V. Lavrik, I. Vlassiouk, Y. S. Puzyrev, V. Parsi Sreenivas, S. T. Pantelides, and K. I. Bolotin, Nat. Commun. **6**, 8789 (2015).
[21] M. K. Blees, A. W. Barnard, P. A. Rose, S. P. Roberts, K. L. McGill, P. Y. Huang, A. R. Ruyack, J. W. Kevek, B. Kobrin, D. A. Muller, and P. L. McEuen, Nature (London) **524**, 204 (2015).
[22] J. H. Los, L. M. Ghiringhelli, E. J. Meijer, and A. Fasolino, Phys. Rev. B **72**, 214102 (2005).
[23] L. D. Landau and E. M. Lifshitz, *Theory of Elasticity* (Oxford Pergamon, Oxford, 1970).
[24] J. A. Aronovitz and T. C. Lubensky, Phys. Rev. Lett. **60**, 2634 (1988).
[25] J.-P. Kownacki and D. Mouhanna, Phys. Rev. E **79**, 040101 (R) (2009).
[26] M. J. Bowick, S. M. Catterall, M. Falcioni, G. Thorleifsson, and K. N. Anagnostopoulos, J. Phys. I (France) **6**, 1321 (1996).
[27] M. Bowick, A. Cacciuto, G. Thorleifsson, and A. Travesset, Phys. Rev. Lett. **87**, 148103 (2001).
[28] E. Cadelano, P. L. Palla, S. Giordano, and L. Colombo, Phys. Rev. Lett. **102**, 235502 (2009).
[29] G. Cao, Polymers **6**, 2404 (2014).
[30] D. Sanchez-Portal, E. Artacho, J. M. Soler, A. Rubio, and P. Ordejon, Phys. Rev. B **59**, 12678 (1999).
[31] R. Nicklow, N. Wakabayashi, and H. G. Smith, Phys. Rev. B **5**, 4951 (1972).
[32] L. J. Karssemeijer and A. Fasolino, Surf. Sci. **605**, 1611 (2011).
[33] M. R. Begley and T. J. Mackin, J. Mech. Phys. Solids **52**, 2005 (2004).
[34] S. P. Timoshenko and S. Woinowsky-Krieger, *Theory of Plates and Shells* (McGraw-Hill, New York, 1951).